Unaveraged simulations of a cavity based free electron laser

Pornthep Pongchalee [a,b,c,*], Brian W.J. McNeil [a,b]

[a] *Department of Physics, University of Strathclyde, Glasgow, G4 0NG, UK*
[b] *Cockcroft Institute, Warrington, WA4 4AD, UK*
[c] *ASTeC, STFC Daresbury Laboratory, Warrington, WA4 4AD, UK*

ARTICLE INFO

ABSTRACT

The computer simulation of a cavity-based (oscillator) Free-Electron Laser (FEL) requires the modelling of both the electron-light interaction in the FEL undulator and the radiation propagation within the optical cavity. The unaveraged 3D FEL simulation code Puffin has been coupled with the Optical Propagation Code (OPC) to allow a broadband, high temporal-resolution cavity FEL to be modelled for the first time. This requires the translation of the radiation field formats between the Puffin and OPC codes. This translation is described and the coupled codes are then used to model an example of a Regenerative Amplifier FEL operating in the VUV.

Introduction

In order to model a Free Electron Laser operating in an optical cavity (oscillator), two simulation codes are usually required: one code to model the FEL interaction in the undulator system, and one to model the radiation propagation within the optical cavity.

Several 3D FEL simulation codes, such as Genesis 1.3 [1], can be used to model the FEL interaction based on the Slowly Varying Envelope Approximation (SVEA). However, Puffin [2,3] (available from [4]) is an unaveraged FEL code that does not apply the SVEA approximation and does not use undulator period averaging of the electron trajectories. The radiation field retains the fast-oscillating term and allows the modelling of broadband (few cycle radiation field) and more complex electron dynamics. This paper describes how such unaveraged modelling can be achieved in a FEL oscillator system.

Previously, the FEL simulation code Genesis 1.3 has been used with the Optical Propagation Code (OPC) [5,6] (available from [7]), to simulate a cavity based Regenerative Amplifier FEL operating in the VUV, by using both codes sequentially within the optical cavity [8]. OPC includes 3D mirror reflection and free-space propagation through the optical path of the cavity.

Here, OPC is used to model the optical propagation inside a cavity while the unaveraged FEL interaction is modelled using Puffin. This paper first describes the translation of the optical field between the Puffin and OPC code formats, necessary for linking the output of the radiation from one code into the other. The translation code is available here [9].

When designing a FEL oscillator to operate at shorter wavelengths towards the X-ray, the optical components used to create the cavity can

be a limiting factor due to their reduced reflectivity, higher absorption, and also lack of tunability when using e.g. Bragg reflectors. The Regenerative Amplifier FEL (RAFEL) uses a sub-saturation, high-gain FEL undulator system together with a reduced optical feedback cavity to obtain FEL saturation in a few cavity round-trips. The RAFEL typically uses low reflectivity mirrors for the optical cavity and can operate into the short wavelength regime [10]. An overview of RAFEL operation over a wide range of parameters in the 1D limit is given in [11].

A RAFEL design operating in the VUV at ∼65 nm is then modelled. The optical cavity was designed to satisfy the cavity stability condition and to match the undulator and cavity lengths to the electron beam repetition rate.

Format conversion

The Puffin radiation field data consists of a 4D array in a HDF5 (.h5) file format with a dimension of $(2, n_z, n_y, n_x)$ describing two orthogonal x and y polarised 3D fields, with n_z representing the direction of field propagation. A schematic illustrating the format conversion for a short Gaussian pulse is shown in Fig. 1. It is seen that the Puffin output field includes the 'fast' oscillatory terms of the radiation for both x and/or y polarisations, so that both planar and circular polarisations may be converted.

While Puffin uses a single HDF5 file to store the radiation field, OPC uses two files. The first is the field in a binary data format as used in the Genesis (.dfl) field file [1]. Each data point consists of an 8-byte (64-bit) floating number which is stored in a 1D array. The size of the array is the product of the number of grid points in x, y and z, with
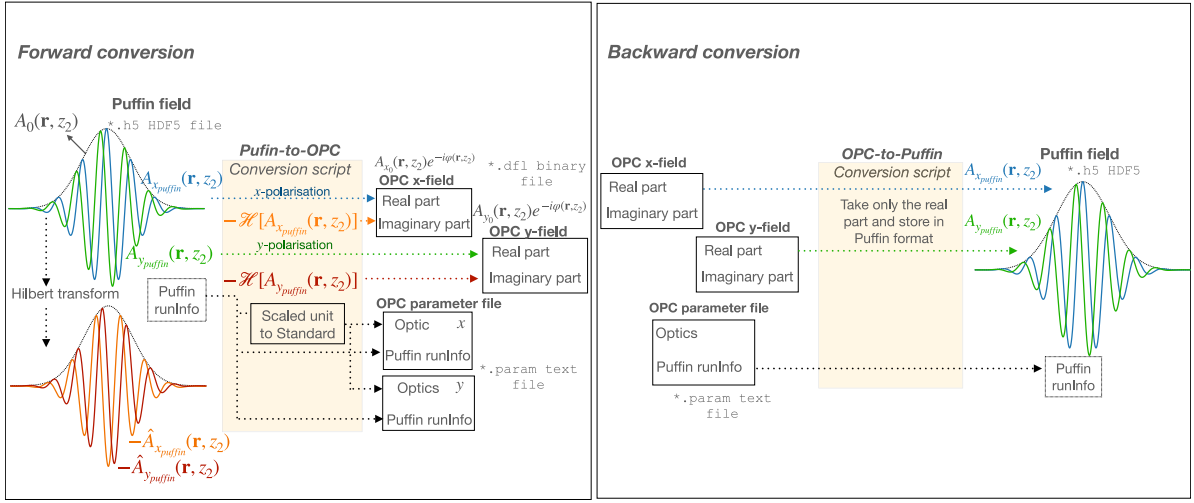

Fig. 1. The format of the Puffin output radiation field and the conversion methods to and from the OPC radiation field format. Left: Puffin-to-OPC and Right: OPC-to-Puffin.

grid-size parameters, number of slices in z etc, stored in a second OPC parameter (.param) text file. The transverse optical field data consists of two of a complex number, which interleave in the array by odd and even indices of the 1D data array. For the temporal information in the OPC data, the number of slices defines the additional axis of the array corresponding to the z-direction of the optical propagation.

The Python conversion script from the Puffin to OPC file format begins by considering the envelope of the optical field in its complex form. The conversion method treats both x and y polarisation of the Puffin field independently. For a simple plane wave, the radiation field of a single polarised orientation that would be obtained from Puffin can be written in Eq. (1) as:

$$A_{puffin}(\mathbf{r},t) = A_0(\mathbf{r},t)\cos(kz - \omega t + \phi(\mathbf{r},t)), \tag{1}$$

where A_{puffin} is the scaled radiation field with amplitude A_0, radiation wave number k, angular frequency ω and phase ϕ. An analytic form is then used to translate the real-value field A_{puffin} into the complex representation of the OPC field format by using a Hilbert transform [12], which also has the effect of shifting the phase of the original signal by $-\pi/2$. The Hilbert transform, denoted by a 'hat', of the Puffin field can then be written as:

$$\begin{aligned} \hat{A}_{puffin}(\mathbf{r},t) &= \mathcal{H}[A_{puffin}(\mathbf{r},t)] \\ &= A_0(\mathbf{r},t)\sin(kz - \omega t + \phi(\mathbf{r},t)) \end{aligned} \tag{2}$$

The OPC envelope is then constructed from the original Puffin field via its Hilbert transform, as:

$$\begin{aligned} \tilde{A}_{opc}(\mathbf{r},t) &= A_{puffin}(\mathbf{r},t) + i\hat{A}_{puffin}(\mathbf{r},t) \\ &= A_0(\mathbf{r},t)\exp[i(kz - \omega t + \phi(\mathbf{r},t))] \end{aligned} \tag{3}$$

In this way, $A_{puffin}(\mathbf{r},t) = \text{Re}(\tilde{A}_{opc}(\mathbf{r},t))$.

In practice, Puffin stores the radiation field data as a function of $z_2 = (ct - z)/l_c$, where $l_c = \lambda_r/(4\pi\rho)$ is the cooperation length, λ_r is the resonant radiation wavelength and ρ is the FEL parameter [2]. When converting the Puffin field into the OPC format, the negative imaginary part must therefore be used so that:

$$\begin{aligned} \tilde{A}_{opc}(\mathbf{r},z_2) &= A_{puffin}(\mathbf{r},z_2) - i\hat{A}_{puffin}(\mathbf{r},z_2) \\ &= A_0(\mathbf{r},z_2)\exp[i(z_2/2\rho - \phi(\mathbf{r},z_2))] \end{aligned} \tag{4}$$

The parameters describing the grid size, number of grid points etc, in both transverse and temporal directions, are then calculated from the Puffin scaled parameters as described in [2], into the OPC scaling, and written into the OPC parameter text file.

For the backward conversion from OPC binary format to Puffin HDF5 format, the process extracts the real part of the OPC data file then reads the number of grid points, grid size etc. from the OPC parameter text file, and writes these into the Puffin HDF5 file format.

Simulation parameters

In the simulation presented here, a steady-state (non-pulsed) interaction is assumed, and the parameters used are similar to those of the 4GLS conceptual design report [13] for a RAFEL operating in the VUV. The electron beam energy is 600 MeV with Gaussian energy spread $\sigma_E = 0.01\%$ with a peak current $I = 355$ A and a normalised beam emittance of $\epsilon_{x,y} = 2$ mm-mrad. The matched transverse electron beam size in the undulator with natural focusing is given by:

$$\sigma_{x,y} = \sqrt{\frac{\epsilon_{x,y}\lambda_u}{\sqrt{2}\pi a_w}}, \tag{5}$$

where λ_u is the undulator period, and a_w is the RMS undulator parameter.

A helical undulator of length 12 m, consisting of 200 periods of wavelength $\lambda_u = 6$ cm, and an undulator parameter of $a_w = 1.414$ gives a resonant radiation wavelength of $\lambda_r = 65.28$ nm and matched transverse electron beam size of $\sigma_{x,y} = 138$ μm. The electron beam FEL parameter is $\rho = 0.002487$ and a gain length of $l_g = \lambda_w/4\pi\rho = 1.92$ m to give a 1D scaled length in the high gain regime of $\bar{z} = 6.25$ [11].

The round-trip cavity length, L_{cav} is set to match the electron bunch repetition rate, f_{rep} and is given by:

$$L_{cav} = \frac{c}{2f_{rep}}. \tag{6}$$

A stable symmetrical cavity is used in this simulation to demonstrate simple RAFEL operation, where the radius of curvature is the same for both mirrors, $(R_1 = R_2 = R)$. In this case, the optical waist position is located at the centre of the cavity where the waist size is given by:

$$w_0^2 = \frac{\lambda_r}{2\pi}\sqrt{L_{cav}(2R - L_{cav})}. \tag{7}$$

At a position z from the cavity centre the optical beamwaist size is then:

$$w(z) = w_0\left(1 + \left(\frac{z}{z_R}\right)^2\right), \tag{8}$$

where z_R is the Rayleigh range:

$$z_R = \frac{\pi w_0^2}{\lambda_r}. \tag{9}$$

From Eqs. (7) and (9), the radius of curvature of both mirrors is then:

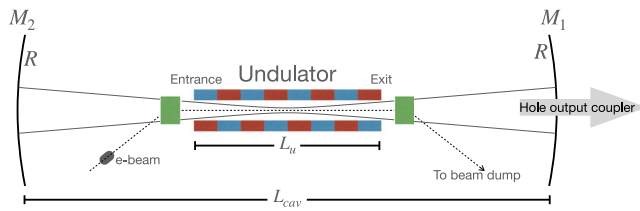$$R = \frac{2z_R^2}{L_{cav}} + \frac{1}{2}L_{cav}. \tag{10}$$

Fig. 2. Schematic of the RAFEL used in the simulation. The cavity of length L_{cav} uses two spherical mirrors with the same radius of curvature R and of reflectivity r. The optical waist is positioned at the centre of the cavity, coincident with the centre of the FEL undulator of length L_u. The upstream mirror uses a hole for out-coupling of the radiation.

In the RAFEL cavity, the optical waist size is matched to the electron beam transverse size to obtain optimum coupling and is given by:

$$w_0 = \sqrt{2}\sigma_{x,y} \tag{11}$$

The RAFEL needs only a small optical feedback cavity to achieve optimum output [11]. The layout of the undulator and optical cavity used here is shown in Fig. 2. The cavity length is set to $L_{cav} = 34.62$ m to match the electron pulse repetition rate of 4.33 MHz. The simulation takes the output field of Puffin from the undulator exit translates it into its OPC format, as described above, which then propagates it via the cavity mirrors M_1 and M_2 back to the undulator entrance, where it is transformed back to the Puffin format to seed the next incoming electron pulse.

The radiation is first reflected off mirror M_1 with radius of curvature $R = 17.5$ m, as calculated from Eq. (10), so that its focal length is $17.5/2 = 8.75$ m. It is placed 11.31 m away from the undulator exit with a 1.0 mm diameter out-coupling hole. The second mirror, M_2, before the undulator entrance, has a radius of curvature the same as M_1 for a symmetrical cavity with concentric configuration, i.e. it forms a stable resonator. The reflectivity of the mirrors used in this simulations here are in a range of $r = 20\%$ to 60%. The RAFEL operation should then reach saturation within a relatively few cavity round-trips [8,11].

The design parameters used here offers a straightforward representation of the integration of the Puffin and OPC simulation codes. 3D simulations were conducted using a steady-state method which applies periodic boundary conditions to the (constant current) electron beam and radiation over an integer number of radiation wavelengths. This means that, while optical diffraction is modelled, pulse effects, such as the electron pulse length, slippage, and cavity detuning, are neglected here. A more in-depth understanding of pulse effects may be found in [14], which describes full 3D, short-pulse simulations, of an Infra-Red FEL oscillator operating with sub-wavelength cavity detunings.

Example simulation

The above Puffin-OPC radiation field conversion method is now tested in a simple steady-state RAFEL configuration, as described by the above parameters. The simulation uses a steady-state periodic boundary window of 10 radiation wavelengths, and starts up from the Puffin simulation of the shot-noise of the electron beam as the spontaneous radiation source in the first pass through the FEL undulator. The spontaneous radiation output from the Puffin code is then converted into the OPC format as described above. The grid sizes of the two codes must be matched at the beginning of the simulation setup. The OPC main input file contains all of the optical path and the optical elements, i.e. mirrors, and output coupling hole. The converted field then propagates through the optical cavity system using OPC via free-space propagation and the two mirrors M_1 and M_2 back to the undulator entrance. This field at the undulator entrance is then converted from OPC format back into
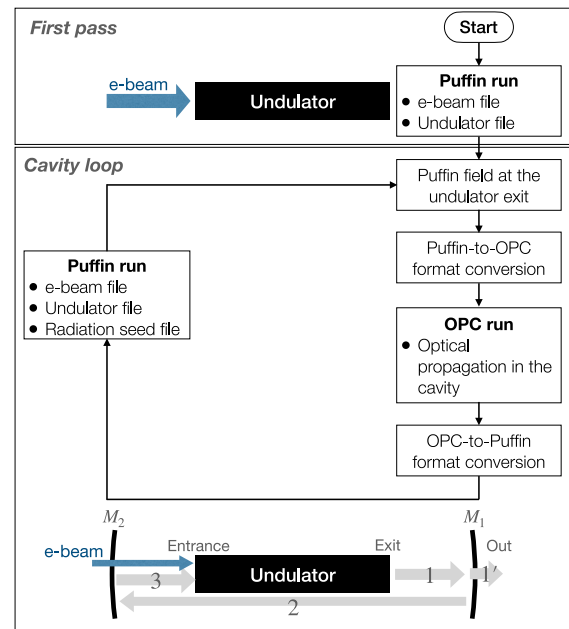

Fig. 3. The schematic shows the flow chart of the RAFEL simulation. It begins with the first pass, Puffin to OPC conversion script, and then enters the cavity loop which is a simple Bash shell script. (1) is the radiation propagation from the undulator exit to M_1 using OPC with a hole out-coupling diagnostic point (1′). (2) The OPC propagation of the reflected radiation at M_1 to M_2. (3) The OPC propagation from M_2 to the undulator entrance where the field is converted to Puffin format and is used as the radiation seed field for the next pass through the undulator.

Puffin format and used as the radiation seed file in the Puffin main input file for the next pass through the FEL undulator. The process runs sequentially, as shown in Fig. 3.

The simulation output of the 10-wavelength periodic optical field as a function of z_2 and the scaled transverse intensities at different points through the cavity are shown in Fig. 4 . It is seen that the simulation using Puffin and OPC maintains the fast-oscillating term of the radiation field in z_2. The diffraction of radiation through the cavity-undulator system, and the radiation output from the hole out-coupling mirror M_1, are all clearly visible.

The RAFEL operation can be analysed via the hole out-coupled radiation pulse energy as plotted in Fig. 5. Note that the output includes all losses that can occur in the system such as, cavity diffractive losses, mirror reflectivity losses, and out-coupling losses. The results demonstrate that there is sufficient optical feedback to achieve saturated RAFEL operation for mirror reflectivities of $r = 20\%, 40\%$, and 60% for both mirrors M_1 and M_2, and for the output mirror M_1's out-coupling hole of diameter 1.0 mm. The RAFEL system is seen to saturate at around 5 to 15 round-trips for decreasing mirror reflectivities. The similar saturated energy outputs for the two higher reflectivities, $r = 40\%$ and 60%, and the lower energy for $r = 20\%$, are consistent with the previous results of [8], which used no hole-output coupling in the cavity.

Conclusion

The unaveraged FEL Puffin and OPC optical simulation codes are now able to be used together in FEL simulations requiring optical components, such as a cavity-based FEL oscillator. Conversion scripts have been developed to enable radiation field transfer between the two simulation codes. This was demonstrated by the modelling of a periodic mode (steady-state) model of a VUV-RAFEL design. This will enable the development of FEL models for future potential ultra short-pulse
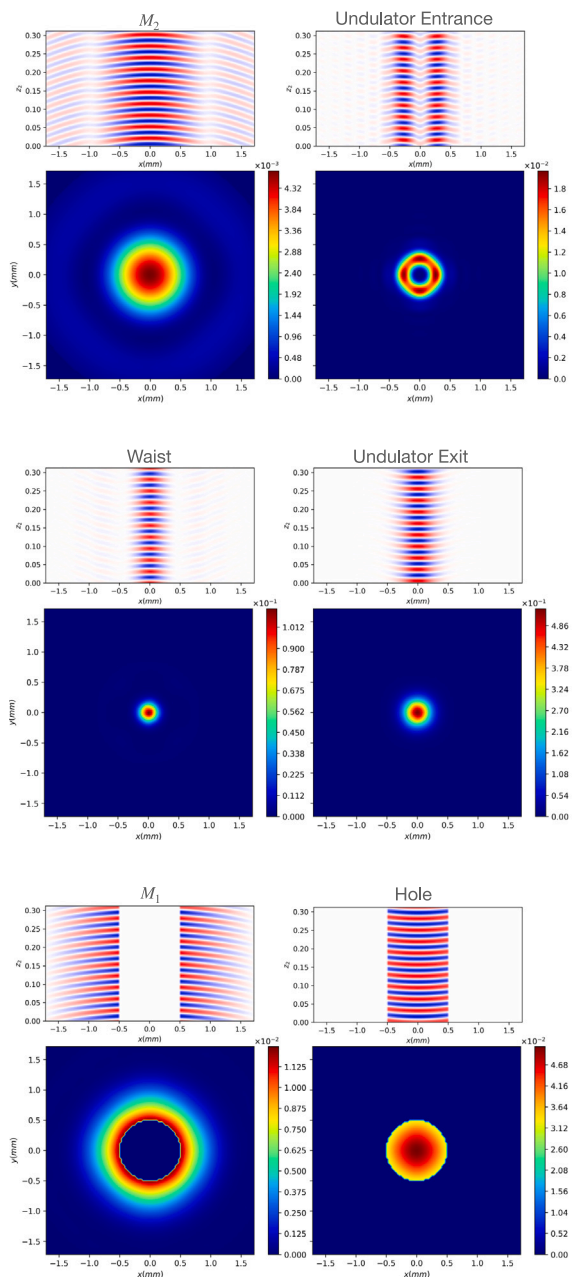
Fig. 4. The steady-state (saturated) radiation field (top sub-plots) and the optical transverse intensity (bottom sub-plots) at different diagnostic positions for one pass through the RAFEL. The top sub-plots show the positive (red) and negative (blue) values of the electric field for the 10 wavelength periodic radiation field sample. The plots start from the mirror M_2 (top-left) which is propagated by OPC to the undulator entrance (top right) where it is translated into Puffin format as a seed field. Puffin then models the FEL interaction through the undulator waist (middle left) and to the undulator exit (middle right) where it is translated into OPC format. OPC then propagates it to mirror M_1. Part of the radiation is then transmitted through the output hole (bottom-right). The reflected radiation (bottom-left) is then propagated back to M_2 and the simulation process repeats. (For interpretation of the references to colour in this figure legend, the reader is referred to the web version of this article.)

(few-wavelength), broadband simulations in cavity-based FEL designs. Other, yet to be explored methods, that require the use of unaveraged FEL and optics simulations, should also now be enabled for the first time.
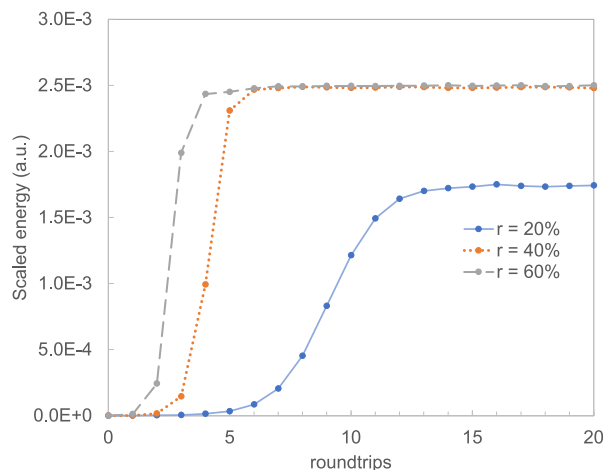
Fig. 5. The RAFEL scaled output pulse energy, as measured at the hole out-coupling, contained within the 10 radiation wavelengths of the steady-state model, as a function of cavity round-trip number. Mirror reflectivities of $r = 20\%, 40\%$ and 60% were used and saturation is seen to occur at around 15, 6, and 5 round-trips respectively.

CRediT authorship contribution statement

Pornthep Pongchalee: Visualization, Software, Methodology, Data curation. **Brian W.J. McNeil:** Writing – review & editing, Supervision.

Declaration of competing interest

The authors declare that they have no known competing financial interests or personal relationships that could have appeared to influence the work reported in this paper.

Data availability

No data was used for the research described in the article.

Acknowledgment

References

[1] Reiche S. GENESIS 1.3: A fully 3D time-dependent FEL simulation code. Nucl Instrum Methods Phys Res A 1999;429(1):243–8. http://dx.doi.org/10.1016/S0168-9002(99)00114-X.

[2] Campbell L, McNeil B. Puffin: A three dimensional, unaveraged free electron laser simulation code. Phys Plasmas 2012;19(9):093119.

[3] Campbell L, McNeil B, Smith J, Traczykowski P. An updated description of the FEL simulation code puffin. In: Proc. 9th international particle accelerator conference. JACoW Publishing; 2018, p. 4579–82.

[4] Campbell L, McNeil B. Puffin: Parallel unaveraged fel INtegrator. 2012, https://github.com/UKFELs/Puffin.

[5] Karssenberg J, van der Slot PJ, Volokhine I, Verschuur JW, Boller K-J. Modeling paraxial wave propagation in free-electron laser oscillators. J Appl Phys 2006;100(9):093106.

[6] van der Slot PJ, Boller K-J. Recent updates to the optical propagation code OPC. In: Proceedings of FEL. 2014, p. 412–5.

[7] Karssenberg J, van der Slot PJ, Volokhine I. Optical propagation code. 2006, https://gitlab.utwente.nl/tnw/ap/lpno/public-projects/Physics-OPC.

[8] McNeil B, Thompson N, Dunning D, Karssenberg J, van der Slot PJ, Boller K-J. A design for the generation of temporally-coherent radiation pulses in the VUV and beyond by a self-seeding high-gain free electron laser amplifier. New J Phys 2007;9(7):239. http://dx.doi.org/10.1088/1367-2630/9/7/239.

[9] Pongchalee P. Conversion scripts between Puffin and OPC field formats. 2023, https://github.com/UKFELs/Puffin-OPC.

[10] McNeil B. A simple model of the free-electron-laser oscillator from low into high gain. Nucl Instrum Methods Phys Res A 1990;296(1):388–93. http://dx.doi.org/10.1016/0168-9002(90)91237-6.

[11] Dunning D, McNeil B, Thompson N. Short wavelength regenerative amplifier free electron lasers. Nucl Instrum Methods Phys Res A 2008;593(1):116–9. http://dx.doi.org/10.1016/j.nima.2008.04.045.

[12] Liu Y-W. Hilbert transform and applications. In: Salih SM, editor. Fourier transform. Rijeka: IntechOpen; 2012, p. 291–300. http://dx.doi.org/10.5772/37727.

[13] Clarke J, Seddon E. The conceptual design of 4GLS at daresbury laboratory. In: Proc. EPAC. 2006, p. 181.

[14] Pongchalee P, McNeil B. Sub-wavelength effects in a free electron laser oscillator. Opt Express 2023;31(16):26673–84.